Background Intensity Removal in Structured Light Three-Dimensional Reconstruction

Raúl Vargas, Jesus Pineda, and Andrés G. Marrugo
Facultad de Ingeniería
Universidad Tecnológica de Bolívar
Cartagena, Colombia.
agmarrugo@unitecnologica.edu.co

Lenny A. Romero
Facultad de Ciencias Básicas
Universidad Tecnológica de Bolívar
Cartagena, Colombia.
lromero@unitecnologica.edu.co

Abstract

In Fourier Transform Profilometry, a filtering procedure is performed to separate the desired information (first order spectrum) from other unwanted contributions such as the background component (zero-order spectrum). However, if the zero-order spectrum and the high order spectra component interfere the fundamental spectra, the 3D reconstruction precision decreases. In this paper, we test two recently proposed methods for removing the background intensity so as to improve Fourier Transform Profilometry reconstruction precision. The first method is based on the twice piecewise Hilbert transform. The second is based on Bidimensional Empirical Mode Decomposition, but the decomposition is carried out by morphological operations In this work, we present as a novel contribution, the sequential combination of these two methods for removing the background intensity and other unwanted frequencies close to the first order spectrum, thus obtaining the 3D topography of the object. Encouraging experimental results show the advantage of the proposed method.

1. Introduction

Fringe projection is a widely used technique based on structured illumination for optical three dimensional (3D) shape measurement. It provides a 3D topography of objects in a non-contact manner, with high resolution, and fast data processing. 3D shape measurement is commonly applied in production automation, robot vision, medical image diagnosis, industrial and scientific applications, cultural heritage and preservation and other fields. Among the existing techniques, Fourier transform profilometry (FTP) is one of the most used techniques [11]. In FTP a filtering procedure is performed to obtain the fundamental frequency spectrum in the frequency domain. This means that frequency aliasing between the zero-order spectrum and the fundamental spectrum has great influence on the measurement accuracy and measurable slope of height variation. If the zero frequency component and the high order spectra component interfere the useful fundamental spectra, the reconstruction precision of FTP will decrease greatly.

To overcome this difficulty various time-space-frequency analysis techniques based on Fourier analysis are often used to filter out background intensity from a single pattern. These techniques include windowed Fourier [6] or Gabor transform [13], wavelet transform [14], and smoothed space-frequency distribution [1]. A major restriction of these methods is their non-adaptive nature. A priori knowledge of parameters like filter window width and basis function is necessary for generating desirable outputs. Other authors have proposed quasi-sinusoidal projection and π-phase shifting for suppressing the zero frequency component and high-order spectra component [9] and composite stripe projection technology for eliminating zero frequency component [3] for improving the accuracy and measurement range of FTP. These techniques have their own applications according to the property of the measured objects. For instance, the π-shifting technique needs to capture two fringe pattern images with π-phase difference to eliminate the background intensity by a subtracting operation. This improves the accuracy and measurement range but is a clear drawback when measuring dynamic objects and scenes.

In this paper we test two recently proposed methods, Morphological-Based Bidimensional Empirical Mode Decomposition (MOBEMD) [15] and the Hilbert Transform [7], for removing the background intensity so as to improve FTP reconstruction precision. In identifying the shortcomings of these two methods we propose the use of both methods sequentially in order to obtain the most accurate 3D reconstruction.

978-1-5090-3797-1/16/$31.00

2. Fourier Transform Profilometry

A sinusoidal grating image is projected onto the object surface (Figure 1). The deformed fringe pattern captured by the CCD can be expressed as

$$g(x,y) = a(x,y) + b(x,y)\cos\left[2\pi f_0 x + \varphi(x,y)\right] \quad , \quad (1)$$

where $a(x,y)$ represents the background illumination, $b(x,y)$ is the amplitude of the cosine function and relates to the contrast of the fringes, f_0 is the carrier frequency, and $\varphi(x,y)$ is the phase that contains the shape information of the tested object. Equation (1) can be rewritten as

$$g(x,y) = a(x,y) + c(x,y)e^{i2\pi f_0 x} + c^*(x,y)e^{-i2\pi f_0 x}, \quad (2)$$

where

$$c(x,y) = \frac{1}{2}b(x,y)e^{i(\varphi_(x,y))} \quad , \quad (3)$$

and superscript $*$ is the complex conjugate of $c(x,y)$. The phase of the fringe system is calculated using the Fourier transform method. Using one-dimensional notation for simplicity, we can express the Fourier transform with respect to x as

$$G(f_x,y) = A(f_x,y) + C(f_x - f_0,y) + C^*(f_x + f_0,y) \quad , \quad (4)$$

where $A(f_x,y)$ and $C(f_x - f_0,y)$ are the 1-D Fourier transforms of $a(x,y)$ and $c(x,y)$. $A(f_x,y)$ represents the zero spectra corresponding to the background component and $C(f_x - f_0,y)$ contains the shape information from the measured object. $\varphi_(x,y)$, $a(x,y)$, and $b(x,y)$ vary slowly compared to the carrier frequency f_0. A properly designed filter is applied to select $C(f_x - f_0,y)$. Equation (5) shows the complex signal obtained by calculating the inverse Fourier transform of $C(f_x - f_0,y)$ [4,7] as

$$c(x,y) = \frac{1}{2}b(x,y)\exp^{i(\varphi(x,y)+2\pi f_0 x)} \quad . \quad (5)$$

The phase $\varphi(x,y)$ can be extracted by computing the logarithm of $c(x,y)$, and then isolating the imaginary part as

$$\varphi(x,y) = \mathrm{Im}\left[\log\left(\frac{1}{2}b(x,y)\right) + i(\varphi(x,y))\right] \quad . \quad (6)$$

The obtained phase is wrapped in the range of π to $-\pi$. A phase unwrapping process is applied to remove the 2π discontinuity. This process is carried out by comparing the wrapped phase at neighboring pixels and adding or subtracting multiples of 2π thus obtaining the continuous phase. This obtained phase can be affected by local shadows, irregular surface brightness, fringe discontinuities and under sampling [10]. In order to overcome these problems, pre-processing strategies are carried out such as binary masks, interpolation techniques and filtering to remove noise, among other.

3. Background Intensity Removal Methods

Frequency aliasing between the zero spectrum and the fundamental spectrum has a great influence on the measurement accuracy and measurable slope of height variation. If the zero frequency component and the high order spectra component interfere the useful fundamental spectra, the reconstruction precision of FTP will decrease greatly. To overcome this problem, we test two methods and propose a variant, based on these two methods, for removing the background intensity so as to improve FTP reconstruction precision.

3.1. Hilbert transform

The Hilbert transform $H(.)$ of a 1D signal $f(x)$ is defined as

$$H(f(x)) = \frac{1}{\pi}\int_{-\infty}^{+\infty}\frac{f(\tau)}{x-\tau} = \frac{1}{\pi x} * f(x) \quad , \quad (7)$$

and the Fourier spectra of $H(f(x))$ is defined as [7]

$$\mathscr{F}\{H(f(x))\} = -j\mathrm{sgn}(w)F(w) \quad , \quad (8)$$

where $\mathrm{sgn}(.)$ is the signum function.

The Hilbert transform can carry out 90 degree phase shifting for the positive frequency and 90 degree phase shifting for the negative frequency. In addition, the DC component is removed.

Luo et al. [7] proposed a piece-wise Hilbert transform to suppress the background intensity of the deformed fringe pattern using only one fringe pattern according to the approximation that the background of the fringes is a slowly varying function and its distribution in each half period of the fringe can be considered as a constant.

The algorithm used to calculate the piece-wise Hilbert transform is the follow:

1. Detect ridges and troughs of the fringes.
2. Calculate the segments of fringe $f_i(x)$ between an adjacent local maximum and local minimum.
3. Calculate twice Hilbert transform (TPHT) to each fringe segment as:
   D1=H($f_i(x)$);
   D11=-imag(D1);
   D2=H(D11);
   D22=-imag(D2);

3.2. Morphological-based BEMD

The deformed fringe pattern is not periodic stationary because the projected sinusoidal pattern is modulated by the tested object. For analyzing non-stationary signals, Bidimensional Empirical Mode Decomposition (BEMD) can

decompose the deformed fringe pattern into Intrinsic Mode Functions (IMF) [5, 8] varying from high frequency to low frequency. Thus, removing the background is a simple operation. However, the decomposition is time consuming. To overcome this problem Zhou et al., [15] proposed a fast algorithm for empirical mode decomposition based on morphological operations and 2D convolution.

After finding the ridges (troughs) by morphological operations the envelopes are estimated by a weighted moving average algorithm and calculated by 2D convolutions to increase the speed of the estimation. The sifting procedure concludes when two modes are extracted, namely, a single IMF and a residue. The IMF corresponds to the fringe pattern without the background.

3.3. MO-BEMD and Hilbert transform

The previous two methods often fail to completely remove the background intensity. MOBEMD estimates the illumination by regions to obtain a global illumination distribution, but it fails to remove all local low frequency components associated with the DC level of each Fringe. In contrast, the Hilbert transform can eliminate these local DC components, but is susceptible to errors when there are global illumination variations, which does not allow a successful maxima and minima detection in the signal.

We propose to use both methods to suppress the background intensity of the fringe pattern. First, with MOBEMD, we obtain a global compensation illumination and then with twice piecewise Hilbert transform a local illumination compensation.

4. Experimental Details

The experimental setup consisted in two parts: a projection system and an observation system (Figure 1). The projection system used was an LED pattern projector (Optoengineering LTPR36-W) that contains a stripe pattern of 400 lines with line thickness 0.01mm. A objective lens of 75-mm focal length was used to project the fringe pattern onto the tested object. The observation system consists of a CMOS camera (Basler Ace with 1280×1024 pixels) that captures the distorted pattern. The captured pattern was analyzed to extract the topographical information of the object. A calibration process was executed to convert the resulting phase map to (x, y, z)-coordinates [2, 12]. The tested object is a dented steel pipe. A dent is a permanent plastic deformation of the circular cross section of the pipe. The dent was produced by means of a Rockwell hardness test, penetrating the pipe with a diamond cone indenter.

In Figure 2 we show the acquired image of the tested object. This image presents a non-uniform illumination distribution and poor contrast of the fringes. Figure 3(a) shows the area of interest for 3D reconstruction. The projected fringes on the edges of the pipe dent exhibit discontinuity

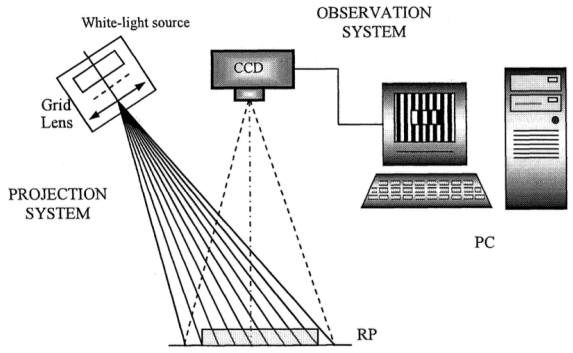

Figure 1. FTP measuring system arrangement.

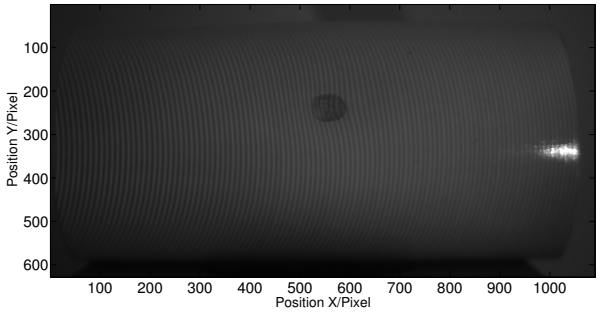

Figure 2. Acquired image of the dented pipe.

problems in some regions that impede an accurate 3D reconstruction.

5. Results and Discussion

5.1. Background Removal

The spectrum in Figure 3(e) was obtained using the FTP method. The unwanted background intensity is mainly represented by the central peak, i.e, the zero-order or DC component. The desired shape information is represented as two peaks centered at the carrier frequency value and its conjugate. A Hanning filter is applied to perform the filtering procedure. The size of the filter was designed to cover most of the frequencies associated with the object, however often leakage frequencies related to illumination or discontinuities in the image lead to incorrect phase information. To overcome this problem, we processed the images for background intensity removal. The results of applying TPHT, MOBEMD and the proposed method (TPHT+MOBEMD) to remove the background intensity are shown in Figures 3(b)-(d). In the second line of Figure 3 we show a profile of the Fourier spectra of the corresponding figures. Figure 3(f) shows the resulting spectrum after applying the TPHT method. This method removes the background intensity variation, however it has problems on compensating illumination in the pipe dent and in addition to generating irregularities at the edges as is shown in Figure 3(b).

Processing the image with MOBEMD provides a more

accurate estimation of the illumination distribution, especially inside the dent, but the overall background is not adequately removed as can be seen in the corresponding Fourier spectrum (Figure 3(g)). Our proposal, of processing the image with MOBEMD+TPHT, leads to an overall uniform intensity with hardly any artifacts in the dent. Figure 3(h) shows the spectrum of TPHT+MOBEMD in which the background is not completely removed but it is negligible.

5.2. Phase Maps and 3D Reconstruction

Accurately retrieving the phase map from the dent is most likely a problem due to the poor contrast and discontinuities of the fringes in the border. The 3D reconstruction is obtained subtracting the estimated linear phase from the reference plane from the continuous experimental phase map. In Figure 4 we show the four 3D reconstructions of the pipe dent. Notice the artifacts in the first three reconstructions (Figures 4(a)-(c)), whereas the reconstruction from the image processed by MOBEMD+TPHT is artifact-free.

To overcome this difficulty, often a binary mask is used, as the one shown in Figure 5(a). The phase unwrapping procedure is carried out without considering the pixels inside the mask. After the continuos phase has been obtained, the phase values of the pixels inside the mask are obtained by interpolation. In Figure 5(b) we show the 3D reconstruction using FTP plus the masking procedure. While this is always a possibility, this leads to inaccuracy in the 3D reconstruction and may altogether fail if the mask is too large relative to the image size.

In Figure 6(a) we show the profiles from the 3D reconstructions along the y-axis passing through the dent. There is a minor offset from the profiles because the reference linear phase is estimated from the experimental image. The preprocessing produces this offset, but it has no influence on the relative z values and the topography. Due to the phase unwrapping problems the profiles from FTP, MOBEMD, and TPHT have reconstruction errors that manifest as spikes. For the sake of comparison, in Figure 6(b) we show the profiles from the 3D reconstruction by FTP, FPT+Mask, and the proposed method. Notice that because of the masking and interpolation, the relatively high slope at the right-side of the spike is much more smooth. This topographical characteristic is preserved with the proposed method.

6. Conclusions

In this work we have presented a typical problem that arises in Fourier Transform Profilometry dealing with uneven illumination and poor contrast of the fringes. This leads to problems in the phase unwrapping stage that produce artifacts in the 3D surface reconstruction. We presented results on real images from a dented pipe using

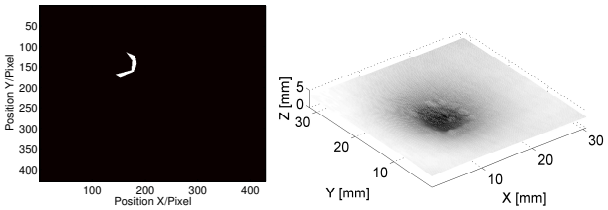

(a) (b)

Figure 5. (a) Binary mask used to avoid phase unwrapping artifact. (b) 3D reconstruction after masking and interpolation.

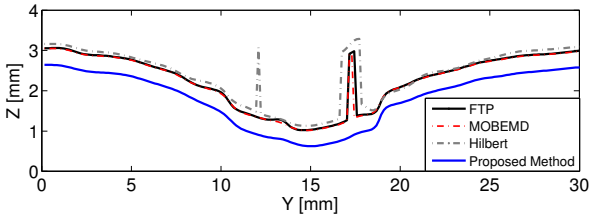

(a)

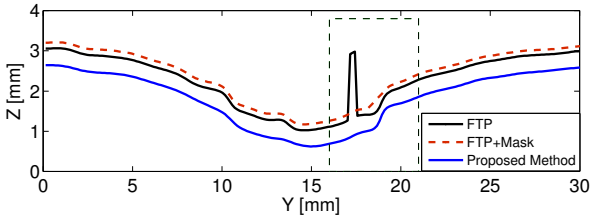

(b)

Figure 6. Profiles from the 3D reconstructions along the y-axis passing through the pipe dent.

three methods for removing the background intensity and improving fringe visibility. The methods MOBEMD and TPHT showed a significant enhancement of the input image, but fail either to adequately compensate the local or overall intensity distribution. For this reason, we proposed to use both techniques, first MOBEMD and followed by TPHT to enhance the images. The proposed method clearly improves the phase unwrapping stage and avoids the use of masks and interpolation which lead to inaccurate 3D reconstruction.

Acknowledgement

This work has been partly funded by Colciencias (Fondo Nacional de Financiamiento para la Ciencia, la Tecnología y la Innovación "Francisco José de Caldas) project 538871552485, and by Universidad Tecnológica de Bolívar project FI1607T2001. The authors thank the support from Dirección de Investigaciones Universidad Tecnológica de Bolívar.

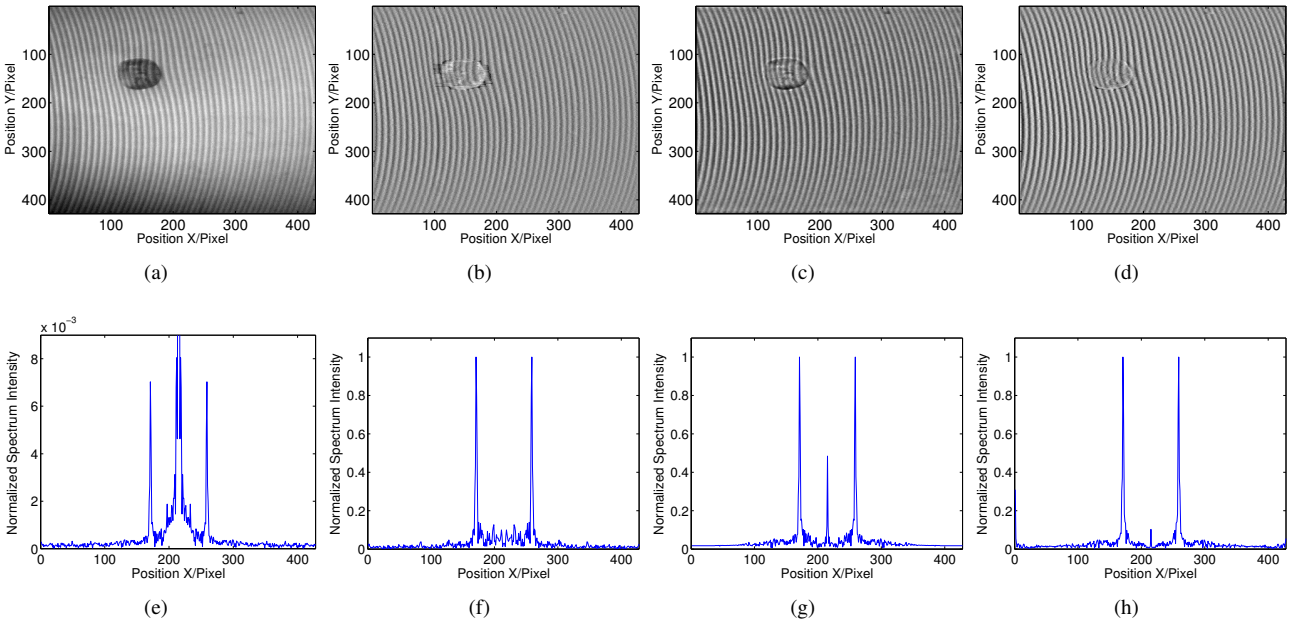

Figure 3. (a) Original image. Background removal with (b) TPHT, (c) MOBEMD, and (d) MOBEMD+TPHT. (e)-(h) A profile of the corresponding Fourier spectra. In (e) the DC component has been truncated for display purposes.

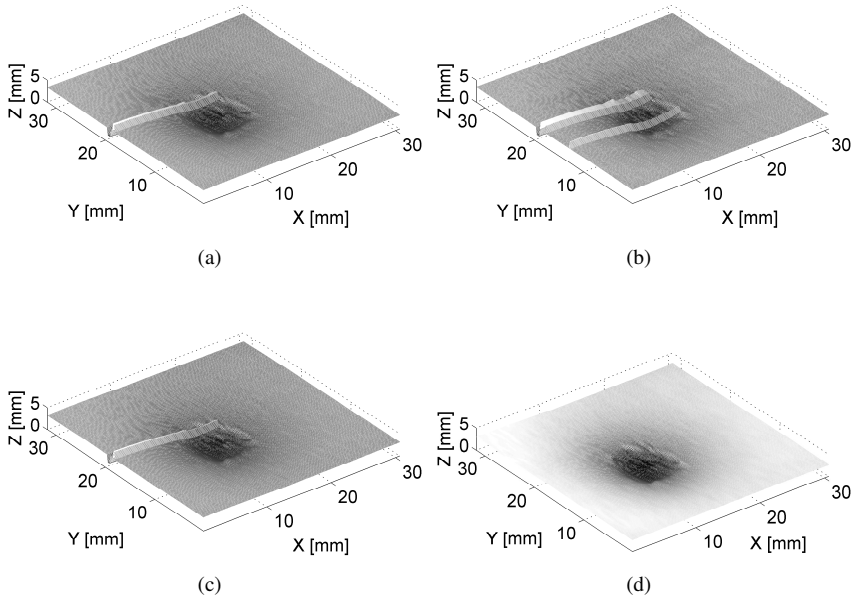

Figure 4. 3D surface reconstruction with (a) FTP, (b) TPHT, (c) MOBEMD, (d) MOBEMD+TPHT.

References

[1] A. Federico and G. H. Kaufmann. Phase retrieval in digital speckle pattern interferometry by use of a smoothed space–frequency distribution. *Applied optics*, 42(35):7066–7071, 2003.

[2] A. L. G. Gómez, J. E. M. Fonseca, and J. L. Téllez. Proyección de franjas en metrología óptica facial. *INGE CUC*, 8(1):191–206, 2012.

[3] C. Guan, L. Hassebrook, and D. Lau. Composite structured light pattern for three-dimensional video. *Optics Express*, 11(5):406–417, 2003.

[4] H. Guo. *3-D shape measurement based on Fourier transform and phase shifting method*. PhD thesis, STATE UNIVERSITY OF NEW YORK AT STONY BROOK, 2009.

[5] N. E. Huang, Z. Shen, S. R. Long, M. C. Wu, H. H. Shih,

Q. Zheng, N. C. Yen, C. C. Tung, and H. H. Liu. The empirical mode decomposition and the Hilbert spectrum for nonlinear and non-stationary time series analysis. *Proceedings of the Royal Society A: Mathematical, Physical and Engineering Sciences*, 454(1971):903–995, Mar. 1998.

[6] Q. Kemao. Windowed fourier transform for fringe pattern analysis. *Applied Optics*, 43(13):2695–2702, 2004.

[7] F. Luo, W. Chen, and X. Su. Eliminating zero spectra in fourier transform profilometry by application of hilbert transform. *Optics Communications*, 365:76–85, 2016.

[8] J. C. Nunes, Y. Bouaoune, E. Delechelle, O. Niang, and P. Bunel. Image analysis by bidimensional empirical mode decomposition. *Image and vision computing*, 21(12):1019–1026, 2003.

[9] X. Su and W. Chen. Fourier transform profilometry:: a review. *Optics and Lasers in Engineering*, 2001.

[10] X. Su and W. Chen. Reliability-guided phase unwrapping algorithm: a review. *Optics and Lasers in Engineering*, 42(3):245–261, 2004.

[11] M. Takeda and K. Mutoh. Fourier transform profilometry for the automatic measurement of 3-d object shapes. *Applied optics*, 22(24):3977–3982, 1983.

[12] J. Villa, M. Araiza, D. Alaniz, R. Ivanov, and M. Ortiz. Transformation of phase to (x, y, z)-coordinates for the calibration of a fringe projection profilometer. *Optics and Lasers in Engineering*, 50(2):256–261, 2012.

[13] J. Zhong and J. Weng. Dilating gabor transform for the fringe analysis of 3-d shape measurement. *Optical Engineering*, 43(4):895–899, 2004.

[14] J. Zhong and J. Weng. Spatial carrier-fringe pattern analysis by means of wavelet transform: wavelet transform profilometry. *Applied optics*, 43(26):4993–4998, 2004.

[15] X. Zhou, A. G. Podoleanu, Z. Yang, T. Yang, and H. Zhao. Morphological operation-based bi-dimensional empirical mode decomposition for automatic background removal of fringe patterns. *Optics express*, 20(22):24247–24262, 2012.